



## Simplified Approach for Torsional Analysis of Non-homogenous Tubes with Non-circular Cross-sections

B. Golami Bazehhour\*, J. Rezaeepazhand

Department of Mechanical Engineering, Ferdowsi University of Mashhad, Mashhad, P.O. Box 91775-1111, Iran

### PAPER INFO

#### Paper history:

Received 20 February 2012

Received in revised form 18 March 2012

Accepted 19 April 2012

#### Keywords:

Torsion

Non-homogeneous

Polygonal Cross-section

Bluntness

### A B S T R A C T

In this paper a method is presented for torsional analysis of non-homogeneous tubes with arbitrarily shaped cross-sections. A previously presented method based on Bredt's theory is extended to achieve formulas for torsional analysis. Shear modulus varies through the thickness according to a power law distribution. To validate the accuracy of the presented formulas for angle of twist and shear stress, calculated results are compared with available analytical and numerical data. Moreover, the effects of thickness, bluntness of corners and cross-sectional shape are investigated. The presented formulas are relatively accurate, simple and applicable to thin to moderately thick cross-sections with constant wall thickness. Based on the method presented herein, one can achieve desirable maximum shear stress and angle of twist for a polygonal non-homogeneous tube using a proper bluntness. The presented formulas quickly converge and can be implemented in optimization programs.

doi: 10.5829/idosi.ije.2012.25.03a.09

## 1. INTRODUCTION

The classical problem of torsion for homogeneous linearly elastic tubes and bars has been extensively investigated by many researchers. However, torsional analysis of bars and tubes when the material is non-homogeneous has received relatively little attention. Functionally graded materials, a new generation of non-homogeneous materials, have gained substantial attention during the past two decades and motivated numerous investigators to devise new solutions for problems involving such materials. Material properties in functionally graded materials have smooth and continuous variation from one surface to another, so that one can take advantage of the properties of its constituents. Functionally graded materials (FGMs) offer the benefits of conventional composites while avoiding the adverse effects of abrupt changes in material properties. In fact, unique characteristics of FGMs are achieved by gradually changing the volume fractions of the constituents through the thickness and therefore, interfacial problems are evaded. Mostly, FGMs are made from ceramics and metals to withstand high temperatures as well as sustaining mechanical loads. These non-homogeneous materials were firstly

manufactured as thermal barriers for aeronautical structures and reactors [1]. However, they are employed in a broad array of applications, such as cutting tools, electronics, biomedical engineering, corrosion and temperature resistant components, etc.

Although the concept of FGM is not very old, a considerable amount of investigations has been reported in different areas, such as heat transfer problems, mechanical response to static and dynamic loads and crack propagation in FGM plates, shells and beams [2]. Furthermore, the torsional analysis of non-homogeneous bars and elements has been of great interest to many researchers since designers and engineers have to deal with torsional loadings in various structures and applications [3]. However, complex cross-sectional shapes of components add complication to formulations and calculations. Such irregular cross-sectional shapes are widely used in various applications in order to satisfy specific considerations like size restrictions and aerodynamic improvements [4]. Several analytical [5-6], numerical [7] and approximate methods [8] have been proposed for torsional analysis of solid and hollow isotropic bars with some simple cross-sections. The complexities of arbitrarily shaped cross-sections make the solution very difficult to deal with. Serra presented an approximate method for torsional analysis of solid bars with arbitrary cross-section using imaginary strips

\*Corresponding Author Email: [be\\_gh92@stu-mail.um.ac.ir](mailto:be_gh92@stu-mail.um.ac.ir) (B. Golami Bazehhour)

and that method was later expanded for hollow bars [9, 10]. The analysis of torsional behavior becomes even more complicated in case of non-homogeneous materials. Functionally graded hollow bars and tubes can be seen in different practical applications that demand superior performance, such as modern biomechanical applications and aerospace structures. Nevertheless, comparatively few papers have been published on the torsion of functionally graded bars and tubes. Lekhnitskii presented a solution for torsion of a non-homogeneous hollow circular cylinder made of a material with cylindrical anisotropy even though he did not specify the material as functionally graded material [11]. Horgan and Chan generalized the classic approach to the torsion problem for a homogenous isotropic bar in terms of the Prandtl's stress function to the inhomogeneous case of a circular rod [12]. Chen founded simple solutions for stress function and torsional rigidity of non-homogeneous circular and elliptical shafts using semi-inverse method [13]. Ecsedi presented a formula for generalized twist of non-homogeneous and anisotropic beams with solid cross-section [14]. He also found a specific elliptical geometry without warping under torsion [15]. Tarn and Chang studied the torsion of elastic FGM bars with emphasis on the end effects [16]. Moreover, torsion of a functionally graded circular cylinder with elastic modulus varying in the axial direction was investigated by Batra [17]. Arghavan and Hematiyan proposed analytical formulas for torsional analysis of functionally graded tubes with shear modulus varying continuously through the thickness according to a power law distribution [18]. They used governing equations in terms of Prandtl's stress function to derive the formulas. Although they assumed the geometry of hollow cross-section to be arbitrary, it only consisted of straight and circular arch curves. In addition, Ecsedi proposed a solution for Saint-Venant torsion problem of solid and hollow cylindrical non-homogeneous bars with shear modulus being a function of the Prandtl's stress function of the same cylindrical bars when the material is homogeneous [19]. Furthermore, Ecsedi and Baksa formulated the Saint-Venant torsion problem for piezoelectric beam in terms of Prandtl's stress function and electric displacement potential function with arbitrary cross-sectional geometry [20]. There are also some other papers on the torsion, buckling and vibration of non-homogeneous tubes and shells which are out of the scope of this paper [21].

The authors of the current paper have previously published a paper which is an extension of Gürel et al.'s model for achieving formulas for torsion of multi-layered tubes with non-circular cross-sections [22]. The layers were assumed to be isotropic with different material properties and thicknesses. However, to the best of authors' knowledge, there has been no report in

the literature to investigate the torsion of arbitrary cross-section FGM tubes with shear modulus changing continuously through the thickness.

In this paper, the modeling of Gürel et al. [10] has been extended to analyze the torsional behavior of FGM tubes. The accuracy of the present approximate formulas is verified and compared with numerical results and some previous works. In addition, the effects of different special non-circular cross-sectional shapes, bluntness of corners, volume fraction of constituents and thickness on the torsional response are investigated. In this study, the materials are assumed to be linearly elastic and tubes are subjected to pure torsion. Moreover, it is assumed that all the examined cross-sections have identical thickness and nominal perimeter. Corners of the considered cross-sections are not very sharp; consequently, the bluntness has roughly the same effect on the stress gradient in proximity of the corners. It will be shown that the presented approximate formulas for shear stress and angle of twist are applicable to thin to moderately thick cross-sections.

## 2. MODEL DESCRIPTION AND FORMULATION

A twisting moment  $T$  is applied to a tube with closed hollow arbitrary cross-section and constant thickness  $t$ . The tube lies in the direction of  $z$ -axis and point  $C$  is the origin of  $x$ - $y$  plane, which is assumed to be the center of rotation of the cross-section. The inner and outer boundaries are denoted by  $\Gamma_{in}$  and  $\Gamma_{out}$ , respectively as illustrated in Figure 1. The cross-section is made of non-homogeneous material with shear modulus varying continuously through the thickness, i.e. from the inner boundary to the outer boundary.

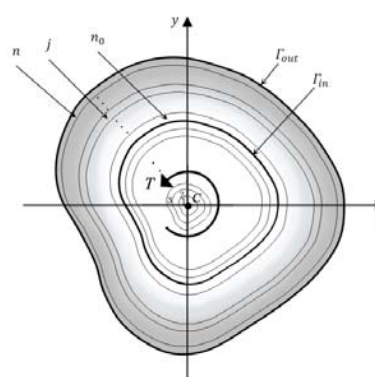


**Figure 1.** Non-homogeneous (functionally graded) cross-section under twisting moment  $T$ , divided by  $n$  imaginary strips.

As previously mentioned, the Gürel et al.'s modeling has been used to derive expressions for shear stress and angle of twist of the tube. In this manner, the whole

domain encompassed by the outer boundary  $\Gamma_{out}$ , is divided into  $n$  imaginary closed strips with the same thickness  $\delta$ . The geometry of the strips is similar to the outer or inner boundary. As depicted in Figure 1, numeration of the imaginary strips starts from the origin of the coordinate system and the first strip of the solid domain of the cross-section is the  $n_0$ th strip and the last strip, accordingly, would be the  $n$ th strip.

The following equations can be obtained from geometric relations between the  $n$ th and  $j$ th strips [10]:

$$A_j = \left(\frac{j}{n}\right)^2 A_n \quad (j = n_0, n_1, n_2, \dots, n) \tag{1}$$

$$dS_j = \frac{j}{n} dS_n \tag{2}$$

$$\delta = \frac{\rho_j(\theta)}{j} \cos(\theta - \beta) \tag{3}$$

$A_n$  and  $A_j$  denote the areas surrounded by the median curves of the  $n$ th and  $j$ th strips, respectively.  $dS_n$  and  $dS_j$  are arch elements corresponding to the same strips and  $\delta$  is the thickness of  $j$ th strip.  $\rho_n$  in Equation (3) is the distance from the point  $C$  to a point on the  $j$ th strip and  $\beta$  is the angle between normal to the curve and horizon ( $\theta=0$ ). These parameters have been delineated in Figure 2.

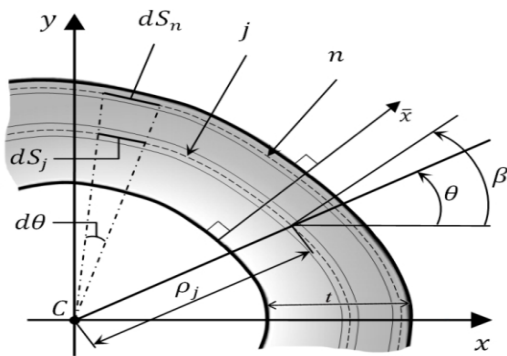


Figure 2. The  $n$ th and  $j$ th strips of the section.

Angle of twist  $\alpha$  of a thin-walled tube subjected to torsional moment  $T$  can be obtained from Bredt's second formula [23]:

$$\alpha = \frac{T}{4GA^2} \oint \frac{dS}{\delta} \tag{4}$$

in which  $S$  is the length of the centerline of the tube and  $G$  is the shear modulus. Assuming that each imaginary strip on the cross-section shown in Figure 1 to be a thin-walled tube, the  $j$ th and  $n$ th strips sustain the partial torsional moments  $\Delta T_j$  and  $\Delta T_n$  from total torsional moment  $T$ , respectively. Therefore, Equation (4) can be written as follows:

$$\alpha_j = \frac{\Delta T_j}{4G_j A_j^2} \oint \frac{dS_j}{\delta} \tag{5}$$

The compatibility condition on the cross-section requires the angles of twist of all the strips to be the same, that is to say,  $\alpha_j = \alpha_n$ :

$$\frac{\Delta T_j}{4G_j A_j^2} \oint \frac{dS_j}{\delta} = \frac{\Delta T_n}{4G_n A_n^2} \oint \frac{dS_n}{\delta} \quad (j = n_0, n_1, n_2, \dots, n) \tag{6}$$

in which  $S_j$  and  $G_j$  are the centerline and the shear modulus of the  $j$ th strip, respectively.  $S_n$  and  $G_n$  are the same quantities for  $n$ th strip. Taking advantage of Equations (1) and (2), Equation (6) can be rewritten as follows:

$$\Delta T_j = \left(\frac{j}{n}\right)^3 \Delta T_n \frac{G_j}{G_n} \tag{7}$$

Total torsional moment  $T$  can be expressed as a summation of all partial moments. Thus, using Equation (7), one can obtain:

$$T = \sum_{j=n_0}^n \Delta T_j = \sum_{j=n_0}^n \left(\frac{j}{n}\right)^3 \Delta T_n \frac{G_j}{G_n} \tag{8}$$

Rearrangement of the above equation gives an expression for the amount of torque carried by the  $n$ th strip in terms of the total torsional moment:

$$\Delta T_n = \frac{T G_n n^3}{\sum_{j=n_0}^n j^3 G_j} \tag{9}$$

As it is obvious, in the problem of pure torsion only shear modulus of the material properties affects the response and comes into the formulation. According to the well-known power law for functionally graded materials, the distribution of shear modulus through the thickness can be expressed as follows [24]:

$$G(\bar{x}) = (G_{in} - G_{out}) \left(\frac{t - \bar{x}}{t}\right)^k + G_{out} \tag{10}$$

where  $G_{in}$  and  $G_{out}$  are the shear moduli at the inner and outer boundaries of the material, respectively (Figure 2).  $k$  ( $0 \leq k < \infty$ ) is the power law exponent and  $t$  is the wall thickness of the cross-section. Increasing the value of  $k$  in Equation (10) increases the volume fraction of the material with shear modulus closer to  $G_{out}$ .

Considering that the segment in Figure 2 is divided into  $(n-n_0)$  imaginary strips, shear modulus of  $j$ th strip can be written using Equation (10):

$$G_j = (G_{n_0} - G_n) \left(\frac{n-j}{n-n_0}\right)^k + G_n \quad (j = n_0, n_1, n_2, \dots, n) \tag{11}$$

Thus,  $G_j$  in Equation (9) can be substituted by the right side expression of Equation (11):

$$\Delta T_n = \frac{T G_n n^3}{\sum_{j=n_0}^n j^3 [(G_{n_0} - G_n) \left(\frac{n-j}{n-n_0}\right)^k + G_n]} \tag{12}$$

Bredt's first formula for tubes under torsion is used to obtain an expression for shear stress on the  $n$ th strip [23]:

$$\tau_n = \frac{\Delta T_n}{2\delta A_n} \quad (13)$$

Replacing Equations (3) and (11) into Equation (13), one can obtain:

$$\tau_n(\theta) = \frac{n^4 T G_n}{2\rho_n(\theta) A_n \cos(\theta - \beta)} \times \frac{1}{\sum_{j=n_0}^n j^3 [(G_{n_0} - G_n) (\frac{n-j}{n-n_0})^k + G_n]} \quad (14)$$

where  $\rho_n(\theta)$  and  $A_n$  are the distance from the point  $C$  to the  $n$ th strip at the angle of  $\theta$  and the area surrounded by the same strip, respectively. For a sufficiently high number of strips, such as  $n=10000, 150000$ , the above equation gives an acceptable solution for shear stress on the  $n$ th strip (outer boundary) at the angle  $\theta$ .

According to the assumption, all the imaginary strips rotate at the same angle. Therefore, the angle of twist of the cross-section would be the angle of twist of the  $n$ th strip. Thus, for angle of twist per unit length  $\alpha$ , Bredt's second formula is used for  $n$ th strip:

$$\alpha = \frac{\Delta T_n}{4G_n A_n^2} \oint \frac{dS_n}{s_n} \quad (15)$$

An infinitesimal arch element on the  $n$ th strip can be expressed in polar coordinates:

$$dS_n = \sqrt{\rho_n^2 + \rho_n'^2} d\theta \quad (16)$$

in which the first derivative of  $\rho_n$  with respect to  $\theta$  is denoted by  $\rho_n'$ . Using Equations (12), (16) and (3) for  $n$ th strip and substituting into Equation (15), one arrives at:

$$\alpha = \frac{n^4 T}{4A_n^2 \sum_{j=n_0}^n j^3 [(G_{n_0} - G_n) (\frac{n-j}{n-n_0})^k + G_n]} \times \int_{\theta=0}^{\theta=2\pi} \frac{\sqrt{\rho_n^2 + \rho_n'^2}}{\rho_n \cos(\theta - \beta)} d\theta \quad (17)$$

So far, formulas for the shear stress on the outer boundary  $\tau_n(\theta)$  and the angle of twist per unit length  $\alpha$  have been obtained. Moreover, by repeating the aforementioned procedure the shear stress on an arbitrary strip, such as  $m$ th strip ( $n_0 \leq m \leq n$ ), can be attained without much difficulty:

$$\tau_m(\theta) = \frac{m^4 T G_m}{2\rho_m(\theta) A_m \cos(\theta - \beta)} \times \frac{1}{\sum_{j=n_0}^n j^3 [(G_{n_0} - G_n) (\frac{n-j}{n-n_0})^k + G_n]} \quad (18)$$

Although the method gives no solution for warping of the cross-section, it provides simple formulas and relatively accurate answers for torsion of thin to moderately thick functionally graded tubes. To show this, other numerical and analytical results are compared with the results calculated from the present method in the section 3. In this study, the normalized shear stress or angle of twist are defined as shear stress or angle of twist of a non-circular tube divided by corresponding values of the similar circular or isotropic tube ( $k=0$ ). It is noteworthy that all of the cross-sections studied here,

have at least two lines of symmetry and thus the center of twist (rotation center) coincides with centroid. Nevertheless, there are some difficulties to find the center of twist in a general case which are associated with the irregularities of the cross-section [25].

### 3. VALIDATION AND RESULTS

The presented formulas are applicable to functionally graded tubes with arbitrary cross-section whose inner boundary is similar to the outer boundary. To validate the formulas, other numerical and analytical results are compared with the results calculated from the presented method in the previous section. In all the following examples tubes undergo a  $1000N.m$  twisting torque.

**3. 1. Circular Cross-section** A circular hollow cross-section tube with inner and outer radii of  $0.06m$  and  $0.1m$ , respectively, is considered. In this case, the outer boundary of the cross-section is divided into sufficient imaginary strips, i.e.  $n=10000$ . Regarding the ratio of inner and outer radii,  $n_0$  becomes 6000. It is obvious from the geometry of the cross-section that  $\theta=\beta$  for all the values of  $\theta$  in Equation (18). Moreover, it is assumed that, shear moduli of inner ( $G_{n_0}$ ) and outer ( $G_n$ ) boundaries are  $90GPa$  and  $150GPa$ , respectively, and the variation of shear modulus is linear ( $k=1$ ).

Figure 3 compares the variation of shear stress across the thickness obtained from Equation (18) with analytical results calculated from the formula presented by Lekhnitskii [11] for a circular cylinder having cylindrical anisotropy. In addition, numerical results are provided using commercial finite element software ANSYS 11. SOLID45 element has been used to model the tubes in FEM analysis. SOLID45 element has 8 nodes and is used for three dimensional modeling of solid components.

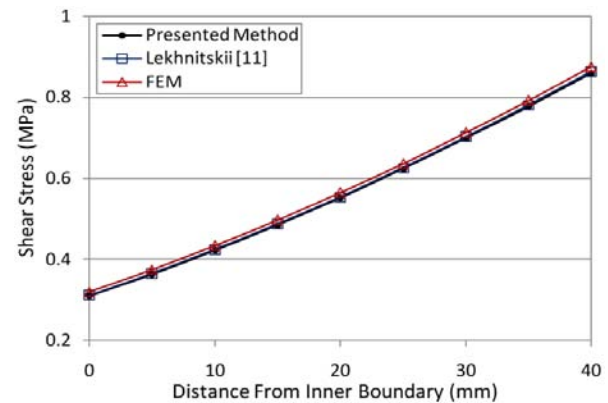


Figure 3. Variation of shear stress through the thickness for circular cross-section.



Mesh sensitivity has been analyzed for all of the tubes to reach convergent and accurate results in FEM software. In this case, results obtained by the present, analytical and numerical methods are in excellent agreement.

**3.2. Flattened Tube** Consider a flattened tube with constant thickness  $t$  which has been previously investigated by Arghavan and Hematyian [18]. Length of straight and radius of arch segments shown in Figure 4 (a) are assumed to be  $L=100mm$  and  $R=50mm$ , respectively. The results from Arghavan and Hematyian [18] and FEM are compared with the results calculated using the present method for  $t=10, 20, 30$  and  $40mm$ . Shear moduli of inner ( $G_{n_0}$ ) and outer ( $G_n$ ) boundaries are  $77GPa$  and  $25.5GPa$ , respectively, and the variation of shear modulus is supposed to be linear ( $k=1$ ). Shear stress is calculated at points A and B. It can be noticed from geometry of the cross-section that these points,  $\theta=\beta=3\pi/2$  in Equation (18). Again the cross-section is divided into  $n=10000$  imaginary strips.

Figures 5 and 6 illustrate the variation of shear stress for different thicknesses at points A and B, respectively.

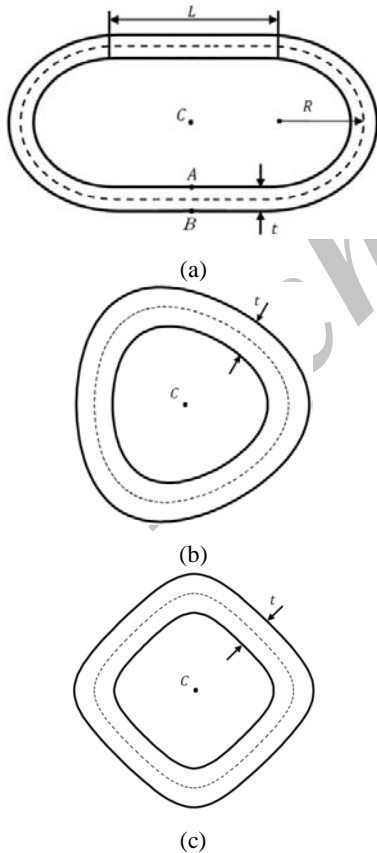


Figure 4. (a) Flattened tube [18], (b) quasi-triangular cross-section and (c) quasi-square cross-section.

As it can be noticed, for cross-sections with thinner thickness, the shear stress calculated using the three methods are close to each other while the discrepancy increases for higher values of thickness. Furthermore, the angle of twist per unit length of the cross-section has been shown in Figure 7. Generally, the observed results provide confidence in the accuracy of the applied approximate solution for torsion of functionally graded tubes.

In the following sections, the effect of different parameters on torsion of functionally graded tubes with specially shaped non-circular cross sections is investigated.

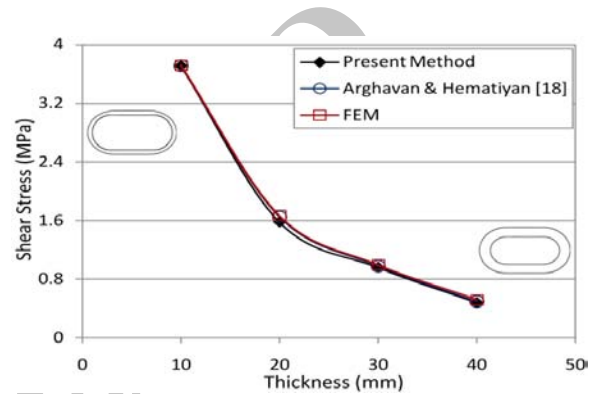


Figure 5. Shear stress at point A.

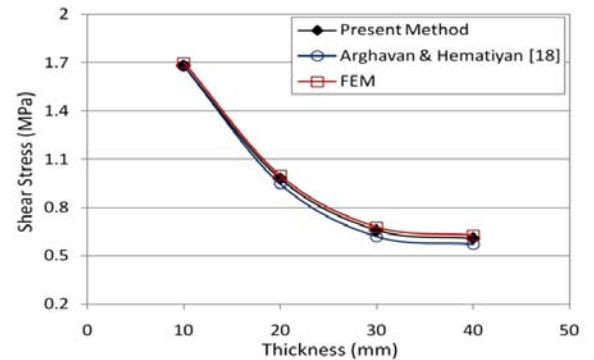


Figure 6. Shear stress at point B.

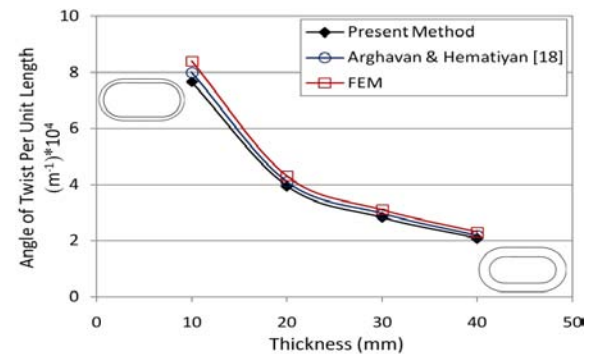


Figure 7. Angle of twist of flattened tubes with different thicknesses.

### 3. 3. Modeling Specially Shaped Cross-section

The special non-circular cross-sections which are considered in this study are polygons with blunted corners. The following mapping functions are used to model such non-circular cross-sections in  $x$ - $y$  plane [26]:

$$x = \lambda(\cos(\theta) + w \cos(N \theta)) \tag{19}$$

$$y = \lambda(c \sin(\theta) - w \sin(N \theta)) \tag{20}$$

in which  $\lambda$  is a real and positive parameter which determines the size of the boundary.  $N$  (integer) specifies the number of sides and  $c$  controls the curve shape while  $w$  changes the bluntness of the corners. Figure 8 presents the effect of the bluntness parameter  $w$  for triangle and square cross sections. Using these equations, one can investigate the effects of different shape parameters on torsional behavior of a variety of cross-sections with tractable shapes. Usage examples of similar non-circular tubes can also be found in fluid ducts [27, 28].

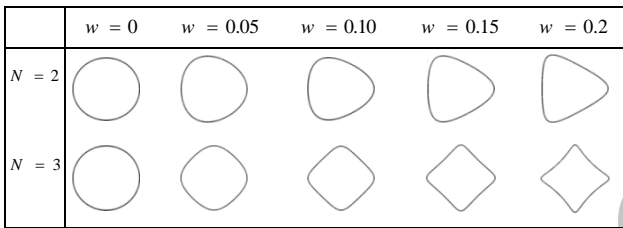


Figure 8. Triangles and squares with  $c=1$  and different bluntness factor ( $w$ ).

#### 3. 3. 1. Quasi-triangular Cross-section

A triangular cross-section with blunted corners has been shown in Figure 4 (b). Corresponding parameters in Equations (19) and (20), are  $w=0.07$ ,  $N=2$  and  $c=1$ . Furthermore, nominal perimeter (dashed curve) of the cross-section is assumed to be constant in the following examples.

In this case, shear moduli of inner ( $G_{n_0}$ ) and outer ( $G_n$ ) boundaries are  $80GPa$  and  $150GPa$  respectively, and the power law exponent is supposed to be  $k=0.25, 0.5, 1, 2$  or  $4$ . The variation of shear stress around the outer boundary of the quasi-triangular cross-section for different values of  $w$  is shown in Figure 9. Clearly, for different bluntness factors, the maximum shear stress occurs in the middle of each side of the cross-section, i.e. at  $\theta=60, 180$  and  $300^\circ$ , rather than at the blunted corners. Moreover, as  $w$  increases, sharper corners, higher shear stresses are produced around the outer boundary of the tube. At all of these points,  $\theta$  is identical to  $\beta$  and, by using Equations (17) and (18) one can obtain the angle of twist per unit length and corresponding shear stresses.

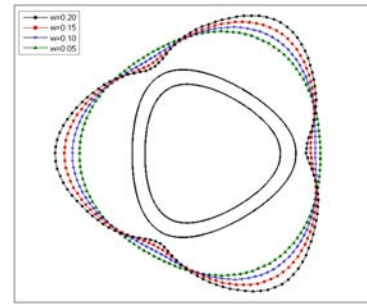


Figure 9. Variation of shear stress around the outer boundary for  $k=1$ .

For comparison, the variations of shear stress around the outer boundary of the same cross-section with  $t=10mm$  and for  $w=0.1$  and  $w=0.2$  have been obtained by the present method and the FEM and shown in Figure 10. Figure 11 illustrates the variation of normalized shear stress ( $\tau/\tau_{k=0}$ ) through the thickness of quasi-triangular tubes for  $t=10mm$ .  $\tau_{k=0}$  represents the shear stress of an isotropic cross-section. It is obvious that increasing the value of  $k$  increases the volume fraction of the material with shear modulus closer to  $G_n$  and, therefore, the shear stress decreases.

Figure 12 illustrates the effect of wall thickness on the angle of twist per unit length of the quasi-triangular cross-section for different values of  $k$ . It can be noticed that for higher values of the wall thickness, the angle of twist is less influenced by distribution of the shear modulus. Figure 13 demonstrates the variation of shear stress through the thickness for  $t=10mm$  which is normalized with respect to the angle of twist ( $\tau/\alpha$ ). As it is seen,  $k$  does not affect the normalized shear stress on the inner and outer boundaries in Figure 13.

In order to investigate the effect of bluntness of corners, a quasi-triangular cross-section with different bluntness factor  $w$  is considered. The power law exponent is assumed to be  $k=1$ . Bluntness factor  $w$  varies from 0 to 0.2 in Equations (19) and (20).

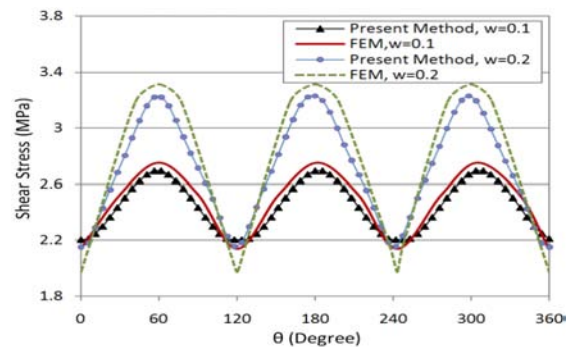
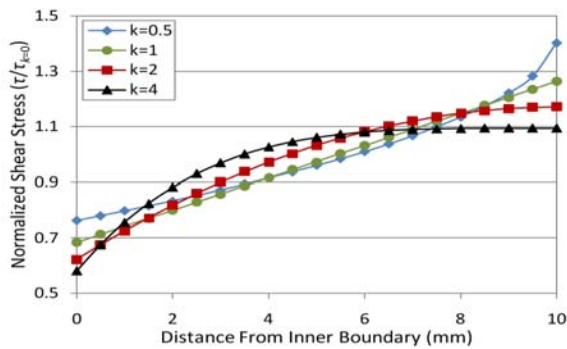
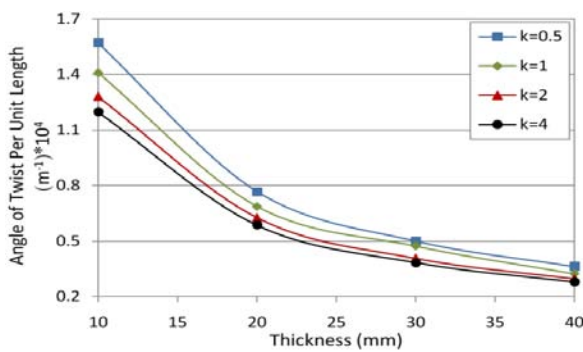


Figure 10. Variation of shear stress around the outer boundary for  $t=10mm$  and  $w=0.1$  and  $0.2$ ,  $k=1$ .



**Figure 11.** Normalized shear stress ( $\tau/\tau_{k=0}$ ) through the thickness for  $t=10mm$  and  $w=0.07$  at  $\theta=60^\circ$ .



**Figure 12.** Angle of twist of quasi-triangular cross-section for different thicknesses with  $w=0.07$ .

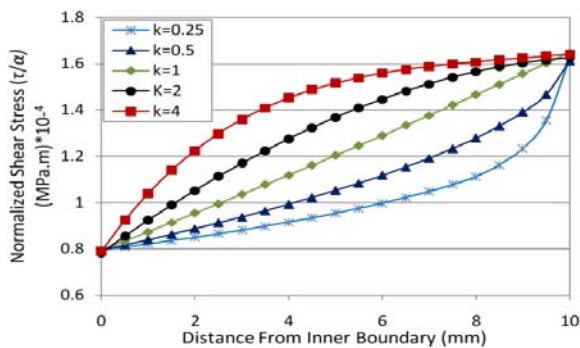


**Figure 13.** Normalized shear stress ( $\tau/\alpha$ ) through the thickness for  $t=10mm$  and  $w=0.07$  at  $\theta=60^\circ$ .

All tubes have identical thickness and,  $\lambda$  of the centerline has been calculated for each cross-section so that the area bounded between the inner and outer boundaries has a constant value in all the cross-sections.

Figures 14 and 15 show the variation of maximum shear stress and angle of twist with bluntness factor ( $w$ ) for quasi-triangular cross-section which are normalized with respect to maximum shear stress and angle of twist of circular cross-section ( $w=0$ ), respectively.

Clearly, the circular cross section ( $w=0$ ) yields the lowest normalized shear stress and angle of twist while changes in bluntness of corners dramatically alter the

value of maximum shear stress and angle of twist. A desirable shear stress or angle of twist for a triangular cross section tube can be achieved when appropriate bluntness is selected for corners of the cross section. In this case, the discrepancy between the presented method and FEM does not exceed 2% for angle of twist and 4% for shear stress.

**3. 3. 2. Quasi-square Cross-section** Figure 4 (c) shows a square cross-section with blunted corners. Corresponding parameters in Equations (19) and (20) are  $w=0.08$ ,  $N=3$  and  $c=1$ . Similar to the previous case, nominal perimeter (dashed curve) of the cross-section is assumed to be constant.

Shear moduli of inner ( $G_{n_0}$ ) and outer ( $G_n$ ) boundaries are  $80GPa$  and  $150GPa$ , respectively, and the power law exponent is assumed to be  $k=0.25, 0.5, 1, 2$  or  $4$ . Similar to the previous case, Figure 16 presents variation of shear stress around the outer boundary of the cross-section for different values of  $w$ . The maximum shear stress happens in the middle of each side of the cross-section, i.e. at  $\theta=45, 135, 225$  and  $315^\circ$  for which  $\theta$  is identical to  $\beta$ . As  $w$  decreases, the square gradually transfers to a circle, and thus, the maximum shear stress reduces while the minimum shear stress, which occurs at the corners, increases and smoother distribution of the shear stress is achieved.

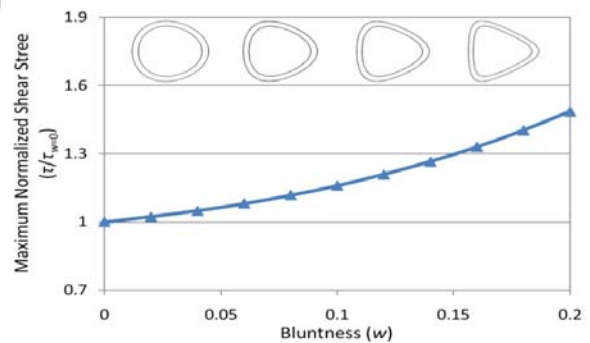


**Figure 14.** Variation of maximum shear stress with bluntness for quasi-triangular tube ( $k=1$ ).

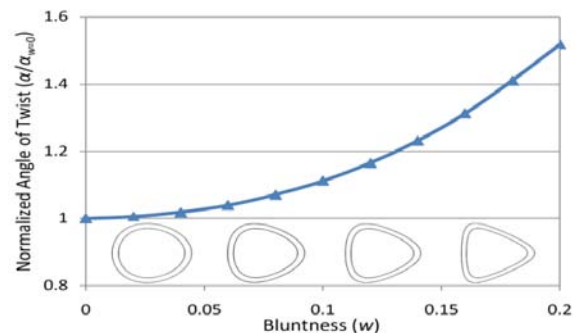


**Figure 15.** Variation of angle of twist with bluntness for quasi-triangular tube ( $k=1$ ).

Figure 17 shows the variation of normalized shear stress ( $\tau/\tau_{k=0}$ ) through the thickness for  $t=40mm$ . Similarly,  $\tau_{k=0}$  represents the shear stress of isotropic cross-section. Angle of twist per unit length of the quasi-square cross-section has been illustrated in Figure 18 for different values of the power law exponent ( $k$ ). As previously mentioned, for thicker cross-sections the angle of twist is less influenced by how the shear modulus is distributed.

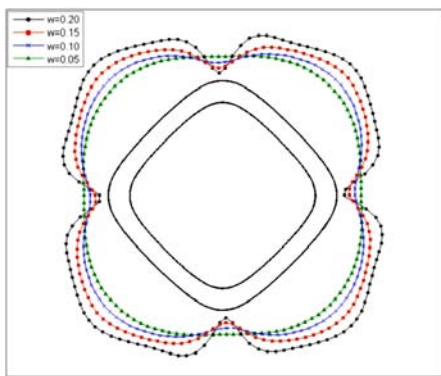


Figure 16. Variation of shear stress around the outer boundary for  $k=1$ .

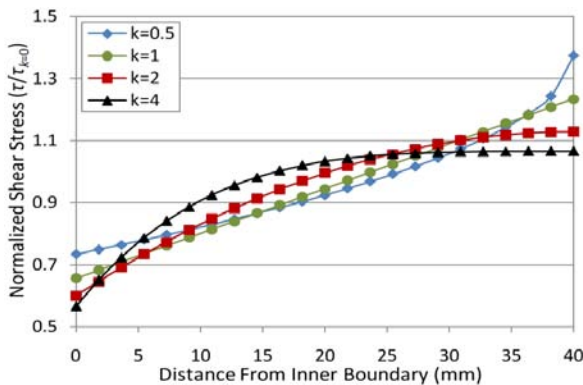


Figure 17. Normalized shear stress ( $\tau/\tau_{k=0}$ ) through the thickness for  $t=40mm$  and  $w=0.08$  at  $\theta=45^\circ$ .

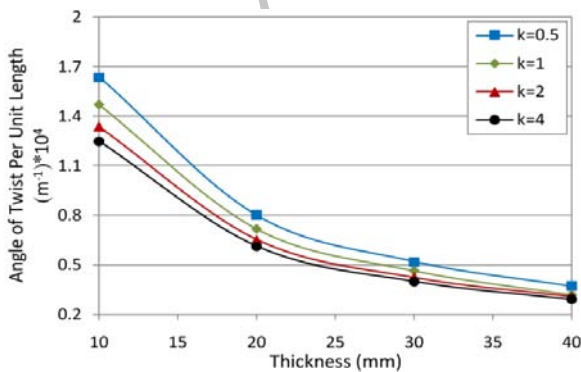


Figure 18. Angle of twist of quasi-square cross-section for different thicknesses with  $w=0.08$ .

Figure 19 presents the variation of shear stress through the thickness for  $t=40mm$  which is normalized with respect to the angle of twist ( $\tau/\alpha$ ). As seen, normalized shear stresses on the inner and outer boundaries do not vary for different values of  $k$  in Figure 19.

Similar to the previous case, to investigate the effect of bluntness of corners, a quasi-square cross-section with variable bluntness factor  $w$  is considered. The power law exponent is assumed to be  $k=1$ .

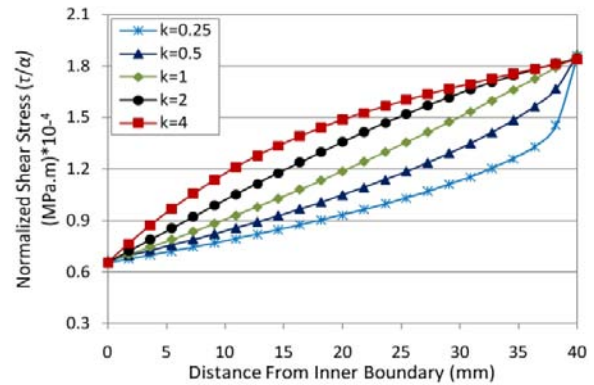


Figure 19. Normalized shear stress ( $\tau/\alpha$ ) through the thickness for  $t=40mm$  and  $w=0.08$  at  $\theta=45^\circ$ .

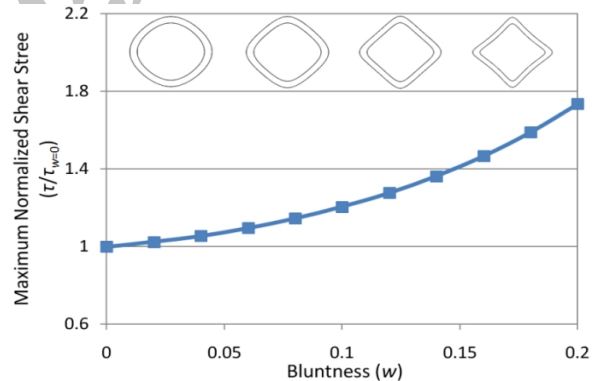


Figure 20. Variation of maximum shear stress with bluntness for quasi-square tube ( $k=1$ ).

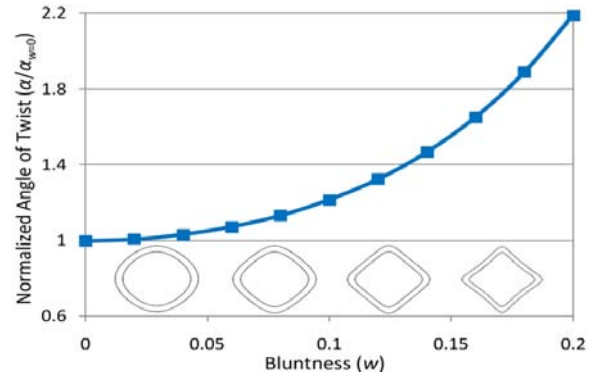


Figure 21. Variation of angle of twist with bluntness for quasi-square tube ( $k=1$ ).



Bluntness factor  $w$  varies from 0 to 0.2 in Equations (19) and (20). The thicknesses of the cross-sections are identical and the  $\lambda$  of centerline has been calculated for each cross-section so that the area bounded between the inner and outer boundaries has a constant value in all the cross-sections. Figures 20 and 21 show the variation of normalized maximum shear stress and angle of twist with bluntness factor ( $w$ ) for quasi-square cross-section. These values are normalized with respect to corresponding maximum shear stress and angle of twist of a circular cross-section ( $w=0$ ), respectively. Similar to the triangular case, by choosing proper bluntness, a designer can considerably reduce the maximum shear stress and corresponding angle of twist of square tubes. In this case, the discrepancy between the presented method and FEM does not exceed 3% for angle of twist and 5% for shear stress.

**3. 3. 3. Effect of Cross-sectional Shape ( $N$ )** In the previous sections, torsional response of quasi-triangular and quasi-square tubes was investigated. The effect of number of sides ( $N$ ) of the cross section on the angle of twist and maximum shear stress is investigated in this section. Using Equations (19) and (20) with  $N=2, 3, 4$  and 5, triangular, rectangular, pentagonal and hexagonal cross-sections can be modeled, respectively ( $c=1$ ). Similar to the previous cases, shear moduli of inner ( $G_{n_0}$ ) and outer ( $G_n$ ) boundaries are assumed to be  $80GPa$  and  $150GPa$ , respectively, and the power law exponent is  $k=1$ . The thicknesses of the cross-sections are identical and the  $\lambda$  of centerline has been calculated for each cross-section so that the area bounded between the inner and outer boundaries has a constant value in all the cross-sections. As can be seen in Figures 22 and 23, increasing  $N$  increases the maximum shear stress and angle of twist. However, this increase becomes more conspicuous for higher values of  $w$ . For a small value of  $w$ , the shape of the cross-section is much closer to a circle. Therefore, the number of the sides ( $N$ ) does not affect the maximum shear stress and angle of twist very much. In contrast, for large values of  $w$ , sharp corners are produced and the maximum shear stress and twist angle increase as the number of the sides increases.

In summury, the results obtained using the presented method demonstrated a good agreement with FEM (ANSYS 11). However, as it can be seen from the previous sections, the difference between the results of the presented method and FEM has increased comparing to that of a circular cross-section. Despite in FEM software, the presented method does not count for cross-sectional warping and its influence on shear stress and angle of twist. Thus, the discrepancy between the two methods increases for non-circular cross-sections. Nevertheless, it must be noted that the presented method

gives a solution for torsion problem of closed cross-sections under uniform pure torsion in which warping effects are usually very small comparing to open cross-sections. Additionally, in order to have more accurate results, it is recommended to apply the method for only thin to moderately thick tubes. Moreover, the power law distribution can be replaced by exponential distribution of material in the formulation. Also similar procedure can be used for torsion problem of multi-layered tubes.

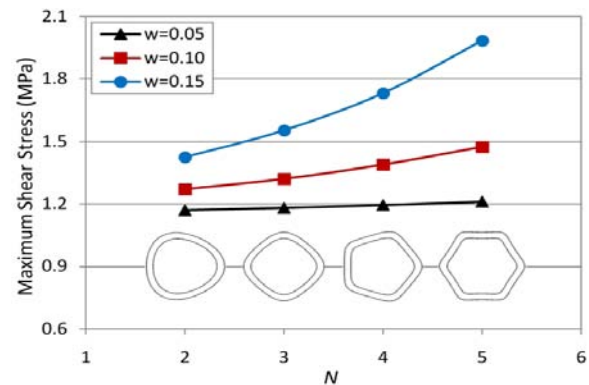


Figure 22. Variation of maximum shear stress for different values of  $N$ .

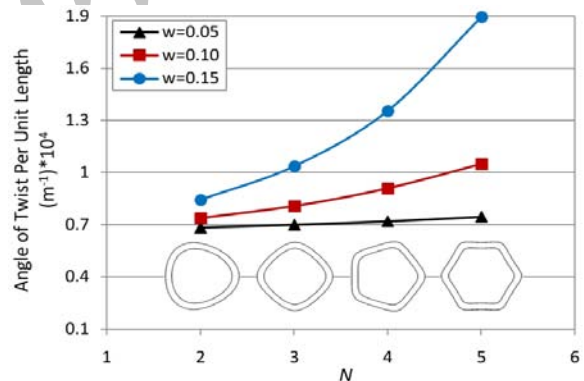


Figure 23. Variation of angle of twist for different values of  $N$ .

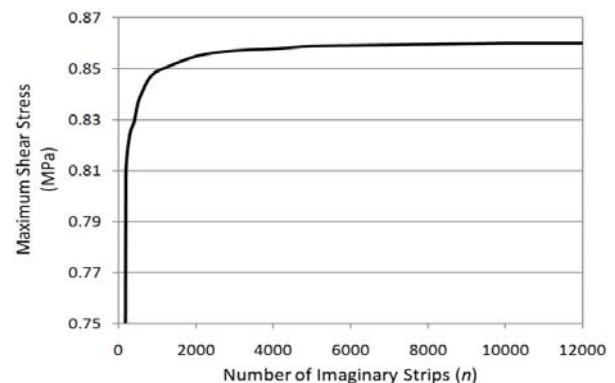


Figure 24. Convergency of the present method.

As mentioned before, the present method gives the convergent results for  $n=10000$ . This fact applies to almost all of the cases studies in this paper. Figure 24 shows the convergency trend of the solution for the quasi-triangular case investigated before.

#### 4. CONCLUSIONS

A relatively simple method was presented for torsional analysis of tubes made of non-homogeneous material with continuous variation of shear modulus through the thickness. The elastic shear stress and deformation of specially shaped polygonal tubes subjected to pure torsion were also examined. In order to verify the accuracy and efficacy of the presented formulas for angle of twist per unit length and shear stress, the obtained results were compared with the available published works and finite element solution. Furthermore, effects of thickness, bluntness of corners and cross-sectional shape on torsional behavior of polygonal tubes were investigated. Based on the results presented herein, the shape and bluntness of the cross-section have a significant effect on the maximum shear stress and angle of twist of a functionally graded tube. It is also concluded that increasing the number of the sides ( $N$ ) in a polygonal cross-section with constant bluntness factor ( $w$ ), increases the maximum shear stress, especially for higher values of  $w$ . Using the present method, one can achieve desirable shear stress and angle of twist for a polygonal functionally graded tube using an appropriate bluntness. The power law exponent ( $k$ ) determines the variation of shear stress through the thickness of the cross-section. For  $k>1$ , the variation of shear stress through the thickness is concave up and for  $k<1$ , the variation of shear stress through the thickness is concave down. Generally, using a proper  $k$ , one can achieve a desired profile of shear stress through the cross-section of an FGM tube. Although the cross-sectional warping is neglected in the method, the presented formulas are well-suited for analysis of thin to moderately thick closed cross-sections in which the warping effects are very small in comparison to that of open cross-sections. The presented simple formulas give convergent results quickly and thus they are appropriate to be used in optimization programs.

#### 5. REFERENCES

- Rooney, F. and Ferrari, M., "Tension, bending, flexure of functionally graded cylinders", *International Journal of Solids and Structures*, Vol. 38, (2001), 413-421.
- Birman, V. and Byrd, L. W., "Modeling and analysis of functionally graded materials and structures", *Applied Mechanics Reviews*, Vol. 60, (2007), 195-216.
- Deshwal, P.S. and Singh, J., "On torsion of cylindrical beams", *Indian Journal of Pure and Applied Mathematics*, Vol. 15, No. 11, (1984), 1261-1271.
- Pantelatos, D.K., Tzotzolakis, D. C. and Mathioulakis, D. S. , "Two noncircular cross-section bodies and a high wing-body configuration at incidence in a low subsonic free stream", *Journal of Fluids and Structures*, Vol. 24, No. 6, (2008), 778-798
- Liu, C. S., "Elastic torsion bar with arbitrary cross-section using the Fredholm integral equations", *Computers, Materials, & Continua*, Vol. 5, No. 1, (2007), 31-42.
- Timoshenko, S.P. and Goodier, J.N., "Theory of elasticity", third ed., McGraw-Hill Book Company, New York, (1970).
- Temis, Y.M. and Karaban, V.V., "Boundary element technique in torsion problems of beams with multiply connected cross-sections", *Journal of KSAIM*, Vol. 5, No. 2, (2001), 39-51.
- Hematiyan, M.R. and Doostfateme, A., "Torsion of moderately thick Hollow tubes with polygonal shapes", *Mechanics Research Communications*, Vol. 34, No. 7-8, (2007), 528-537.
- Serra, M., "Approximated calculus of torsional rigidity of beams with solid cross-section", *Computers & Structures*, Vol. 62, (1997), 771-774.
- Arif Gürel, M., R. Kadir Pekkökgöz and M. Kisa, "An approximate torsion analysis of closed moderately thick-walled, thick-walled, and solid cross-sections", *Turkish Journal of Engineering & Environment Sciences*, Vol. 32, (2008), 277-287.
- Lekhnitskii, S.G., "Theory of elasticity of an anisotropic body", Mir Publishers, Moscow, (1981).
- Horgan, C.O. and Chan, A. M., "Torsion of functionally graded isotropic linearly elastic bars", *Journal Elasticity*, Vol. 52, (1999), 181-199.
- Chen, Y., "Torsion of nonhomogeneous bars", *Journal of the Franklin Institute*, Vol. 277, No. 1, (1964), 50-54.
- Ecsedi, I., "A formula for the generalized twist", *International Journal of Solids and Structures*, Vol. 41, (2004), 4097-4105.
- Ecsedi, I., "Elliptic cross section without warping under twist", *Mechanics Research Communications*, Vol. 31, (2004), 147-150.
- Tarn, J.Q. and Chang, H. H., "Torsion of cylindrical orthotropic elastic circular bars with radial inhomogeneity", *International Journal of Solids and Structures*, Vol. 45, No. 1, (2008), 303-319.
- Batra, R.C., "Torsion of a functionally graded cylinder", *AIAA J*, Vol. 44, (2006), 1363-1365.
- Arghavan, S. and Hematiyan, M. R., "Torsion of functionally graded hollow tubes", *European Journal of Mechanics-A/Solids*, Vol. 28, No. 3, (2009), 551-559.
- Ecsedi, I., "Some analytical solutions for Saint-Venant torsion of non-homogeneous cylindrical bars", *European Journal of Mechanics-A/Solids*, Vol. 28, No. 5, (2009), 985-990.
- Ecsedi, I. and Baksa, A., "Prandtl's formulation for the Saint-Venant's torsion of homogeneous piezoelectric beams", *International Journal of Solids and Structures*, Vol. 47, (2010), 3076-3083.
- Irani, F. and Daniali, S., "Reinforced concrete columns in torsion", *International Journal of Engineering*, Vol. 4, No. 6, (1993), 179-185.
- Gholami Bazehhour, B. and Rezaeepazhand, J., "Approximate torsional analysis of multi-layered tubes with non-circular cross-sections", *Applied Composite Materials*, Vol. 18, No. 6, (2011), 485-497.
- Wang, C. T., "Applied Elasticity", McGraw-Hill, New York, (1953).
- Fotros, F., Pashaei, N.H. and Naei, M.H., "Effect of geometric nonlinearity on stress analysis in large amplitude vibration of thin circular functionally graded plates with rigid core",

- International Journal of Engineering Transaction A: Basics*, Vol. 24, No. 3, (2011), 281-290.
25. Ecsedi, I., "A formulation of the centre of twist and shear for nonhomogeneous beam", *Mechanics Research Communications*, Vol. 27, No. 4, (2000), 407-411.
26. Rezaeepazhand, J. and Jafari, M., "Stress analysis of perforated composite plates", *Composite Structures*, Vol. 71, No. 3-4, (2005), 463-468.
27. Isazadeh, M.A., "Thermal development for ducts of arbitrary cross-sections by boundary-fitted coordinate transformation method", *International Journal of Engineering Transactions A: Basics*, Vol. 15, No. 3, (2002), 211-226.
28. Das, K. and Saha, G., "Pulsatile motion of blood in a circular tube of varying cross-section with slip flow", *International Journal of Engineering Transaction B: Applications*, Vol. 25, No. 1, (2012), 9-18.

## Simplified Approach for Torsional Analysis of Non-homogenous Tubes with Non-circular Cross-sections

B. Golami Bazehhour, J. Rezaeepazhand

Department of Mechanical Engineering, Ferdowsi University of Mashhad, Mashhad, P.O. Box 91775-1111, Iran

### PAPER INFO

چکیده

#### Paper history:

Received 20 February 2012

Received in revised form 18 March 2012

Accepted 19 April 2012

#### Keywords:

Torsion

Non-homogeneous

Polygonal Cross-section

Bluntness

در این مقاله روشی برای تحلیل پیچشی تیوب‌های غیر همگن با سطح مقطع دلخواه ارائه می‌شود. به این منظور روشی موجود که بر اساس تئوری برت می‌باشد بسط داده می‌شود تا فرمول‌هایی جهت تحلیل پیچشی به‌دست آید. مدول برشی در اینجا مطابق با قانون توزیع توانی و در جهت ضخامت دیواره تیوب تغییر می‌کند. به منظور تایید دقت فرمول‌های ارائه شده برای زاویه پیچش در واحد طول و تنش برشی، نتایج محاسبه شده با داده‌های تحلیلی و عددی موجود مقایسه می‌شوند. علاوه بر آن، اثر ضخامت، تیزی گوشه‌ها و شکل هندسی سطح مقطع مورد بررسی قرار می‌گیرند. فرمول‌های ارائه شده به نسبت دقیق، ساده و مناسب جهت تحلیل تیوب‌هایی با جداره نازک تا نسبتاً ضخیم می‌باشند. بر پایه روش ارائه شده در این تحقیق، می‌توان با انتخاب مناسب میزان تیزی (پخ) گوشه‌های سطح مقطع، زاویه پیچش و ماکسیمم تنش برشی مورد نظر را در تیوب‌های غیر همگن با شکل سطح مقطع چند ضلعی به راحتی به‌دست آورد. نتایج در روش ارائه شده به سرعت همگرا می‌شوند و لذا می‌توان از آن در برنامه‌های بهینه‌سازی به راحتی استفاده کرد.

doi: 10.5829/idosi.ije.2012.25.03a.09